Alexandria Engineering Journal (2022) 61, 159–173

HOSTED BY

Alexandria University

Alexandria Engineering Journal

www.elsevier.com/locate/aej
www.sciencedirect.com

# High-dimensional multi-objective optimization strategy based on directional search in decision space and sports training data simulation

Yuan Cao [a], Huaqing Mao [b,*]

[a] Sports Reform and Development Research Center, Institute of Physical Education, Henan University, Kaifeng 475001, Henan, China
[b] School of Computer Engineering, Hubei University of Arts and Science, Xiangyang 441053, Hubei, China

Received 22 February 2021; revised 14 April 2021; accepted 26 April 2021
Available online 5 June 2021

KEYWORDS

Decision space;
High-dimensional multi-objective optimization;
Target space decomposition;
Sports training simulation

**Abstract** In many cases, some programs often have some milestone activities that decision makers need to pay attention to. In this case, managers must efficiently describe these different decision-making spaces and use this as a basis to optimize possible solutions. Choosing a suitable decision-making space has always been a major factor in decision-making management, and it is also one of the key factors that managers must determine when making plans. Multi-objective optimization is to optimize multiple objectives at the same time. Multi-objective optimization algorithms have been widely used in many technology industries. This article researched from two parts: model display and optimization algorithm. The first is to deepen the basic characteristics of project planning and decision-making when there are more decision-making spaces. Based on the existing decision-making network planning methods, combined with the situation analysis method, a decision-making network planning model that can show more decision-making space is established. Secondly, based on the actual improvement requirements, the multi-objective optimization method in the multi-decision network design model and the simulation model of activity exercise data are established. The purpose is to create a relatively complete project planning decision model and optimization algorithm that can select multiple decision spaces at the same time through the above experimental research.



## 1. Introduction

In many cases, some programs often have milestone activities that decision makers need to pay attention to, but other programs do not have milestone activities, which are called milestone activities hereinafter. This milestone activity makes the implementation process of some feasible plans, the natural or

* Corresponding author.
E-mail address: mr.maohuaqing@hbuas.edu.cn (H. Mao).
Peer review under responsibility of Faculty of Engineering, Alexandria University.

https://doi.org/10.1016/j.aej.2021.04.077

social environment and the potential risks they face very different from other plans, so that a set of feasible arrangements in the project plan must be divided into several different decisions. In this case, managers must efficiently describe these different decision spaces and use this as a basis to optimize possible solutions. In essence, this type of program decision can be regarded as a question of how to choose a decision space. In all project management processes, clear macro decision-making can be made, which has a certain guiding role in project decision-making planning. In most of the time, the main job of the manager is to formulate a plan, determine the decision-making plan of the project plan, and then select the specific execution time, implementation cost and resource management of the plan. In other words, choosing a suitable decision-making space has always been a major factor in decision-making management, and this is also one of the key factors that managers must determine when making plans.

There are many multi-objective improvement problems in social activities. Multi-objective improvement is to optimize multiple objectives at the same time. Multi-objective optimization algorithms have been widely used in many technology industries. Generally speaking, if several goals are optimized at the same time, there will be conflicting situations and decisions of the current situation that are most beneficial to the decision maker. Single-objective optimization is to optimize only one objective, so there is only one optimal situation, while multi-objective optimization problems are contradictory in different optimization objectives. Different weights will have different optimal solutions for different goals. Therefore, the multi-objective optimization problem is to give an optimal solution to a group.

In recent years, the decision-making control system has developed by leaps and bounds and has been used in all aspects of society. Among them, activities, exercises and management are all very important applications. Through systematic analysis and research on existing physical activities, exercise and management, combined with computer artificial intelligence theory and existing activity exercise management decision-making, through experiments to simulate exercise training data, find out the decision support in line with the current activity exercise management theory method.

On this basis, this article conducts research from two parts: model display and optimization algorithm. The first is to deepen the basic characteristics of project planning and decision-making when there are more decision-making spaces. Based on the existing decision-making network planning methods, combined with the situation analysis method, a decision-making network planning model that can show more decision-making space is established. Secondly, based on the actual improvement requirements, the multi-objective optimization method in the multi-decision network design model and the simulation model of activity exercise data are established. The purpose is to create a relatively complete project planning decision model and optimization algorithm that can select multiple decision spaces at the same time through the above experimental research.

## 2. Related work

In the decision-making process of project planning and management, network planning methods have been widely used and effectively applied. At present, network planning has developed many different model expression methods in reality: for example, the model expression method in network planning. The CPM optimization thought recorded in the literature [1] uses the network diagram to realize the time and maneuvering time of each operation, and constantly adjusts and improves the network planning. Specific resources allocated to different activities to achieve the best effect or best plan. The PERT method proposed in literature [2] is mainly used to manage the plan of a given project, which has many uncertain factors and process parameters, which cannot be very accurate. This method can cleverly synthesize different expert suggestions, and obtain the optimal solution under uncertain parameters through analysis. Document [3] records that the VERT method is a quantitative analysis method for risk decision-making that combines stochastic network and computer simulation technology. This method is mainly used for risk analysis of certain technical projects with very large uncertainties, such as weapons and equipment research and development, new product development, flood control, rail transit, emergency planning, environmental improvement and other industries. In addition to the GERT method, the document [4] records that the parameter of the GERT process is not only an uncertain variable, but the occurrence of the process itself is also an uncertain situation, which makes the improvement of this type of network model more difficult. Theoretically, the optimization problem of the GERT model, especially the time cost optimization problem has not been fully solved. Compared with other network planning methods, network planning has great advantages in expressing project decision-making issues. The network decision-making planning method, recorded in the literature [5], pointed out that the main routing method of decision-making is a network planning method formed on the basis of the traditional main routing method. This method has the feature of adding some decision points to the overall network planning, indicating that these activities have different possibilities. Literature [6] systematically investigated the network decision-making planning model and optimization function, and proposed the uncertainty in network decision-making and its corresponding graphical representation and optimization algorithm.

When there are more than three optimization goals, it means that there are high-dimensional goals. Due to the strong increase in computational complexity, the calculation of the usual algorithm is relatively slow. Therefore, this article gives some sharing on high-dimensional multimedia optimization problems. At the beginning of this century, literature [7] first proposed a multi-dimensional and multi-objective optimization problem, but because the emergence of new science and technology has greatly promoted the development of this industry, the difficulty of solving it has not been effective until a few years ago. development of. It has been programmed to a new hot spot in the multi-objective optimization industry. In view of the many problems faced by multi-dimensional and multi-objective optimization dimensions under different decision-making needs, the multi-dimensional optimization of the project plan has formulated a number of specific clauses, such as literature [8], to reduce the most time-consuming non-explicit ranking optimization in high-dimensional multi-objectives And various effective sorting methods; the network time cost model based on the electronic data table noted in the document [9]; the project planning time cost balance optimiza-

tion genetic algorithm noted in the document [10]; the document [11] noted The minimum segmentation set for the optimization of time cost balance; the document [12] records the time frame optimization algorithm under fixed resource constraints; the document [13] records the differential development algorithm for network planning, and the document [14] records Automatic interaction model for network planning optimization and capital equilibrium balance; Document [15] records the multi-objective smaller variation method for design optimization decision-making; Document [16] records the multi-objective optimization algorithm for designing network schedules; [17] The record points out the network resource planning balance model; the reference [18] records point out the resource balancing optimization algorithm based on the non-critical process group; the reference [19] records points out the mixed balance of construction project cost management and quality management Optimization algorithm; Document [20] records points out the fuzzy balance sheet optimization method of construction project cost and engineering quality.

Sports simulation: Literature [21] Sports simulation is the use of computer simulation technology to reproduce and simulate the learning experience, training methods, manager's organization plan and athlete's training level of physical trainers or trainers to obtain physical training. Scientific and technological experiments for answering, distinguishing, judging, leading and evaluating situations. The document [22] records that the motion capture technology uses sensors to actually record the human motion in the three-dimensional space, and then the computer instructs the simulated human figure on the screen according to the recorded data. The main feature of this method is that it can record real human motion data. Because the generated action is basically the repetition of the most important human body action, the action image effect is very real and can generate many complicated actions. Document [23] records three typical motion devices: optical devices, electromagnetic devices and mechanical devices. The document [24] records that the working procedures of motion capture include planning and raw data collection, tracking, identification, bone transformation and virtual mapping. Document [25] records that the methods of motion detection include signal processing, mapping offset, mixed motion, texture motion and motion card. The document [26] records that because virtual simulation sports involves virtual situations and simulated people, real-time reproduction and interaction are particularly important in the virtual environment of simulated people. Real-time rendering methods are divided into visibility evaluation, level of detail, and image-based rendering technology. The concept of interaction mainly refers to the entity that interacts between the user and the system through virtual reality, such as the ability to select the physical characteristics of the human body through interaction.

## 3. Research on multi-objective evolutionary optimization method based on decision space search

### 3.1. Directional search strategy based on decision space

#### 3.1.1. Select individuals

NSGA-II is a relatively classic multi-objective evolutionary algorithm, which has a wide range of applications and can help multi-objective optimization algorithms with a simple and commonly used structure [27]. NSGA-II is a multi-objective optimization algorithm based on Pareto advantage. The algorithm first randomly generates a P0 population, uses the binary rotation method for selection and matching, and then generates decomposition Q0 crossover and mutation genetic operations, and the population size is set to N. The parent population Pt and the anti-population Qt are intertwined to form a large population Rt. On the basis of the combined population Rt, select the environment, give the Rt stratification according to the Pareto odds ratio, then calculate the aggregation distance of the critical layer, calculate the individual to obtain the partial order set according to the need, and finally specify the overall according to the partial order ratio Select N individuals in the partial order for the next iteration. The graph is roughly as shown in Fig. 1:

The formula for gathering distance is:

$$P[i]_{distance} = \sum_{k=1}^{r} \left( P[i+1].f_k - P[i-1].f_k \right) \tag{1}$$

#### 3.1.2. Algorithm flow

Decision-based strategy-driven search strategy can be combined with dominance-based algorithms to solve high-dimensional continuous multi-objective optimization problems, and the original algorithm is easy to modify, making it easier to subscribe to DS strategies. Fig. 2 shows the algorithm flow combined with the DS strategy.

### 3.2. Test questions and evaluation indicators

#### 3.2.1. DTLZ test function

The DTLZ test function is a series of popular test questions used to test the execution of multi-objective evolutionary algorithms. The test questions are jointly constructed by Deb et al. and contain different characteristics. This test question is DTLZ1-7, used for experimental comparison. The DTLZ series of problems are multi-objective continuous optimization problems. In this test series, the number of optimization goals and the number of decisions can be used as parameters and can be changed through algorithm testing [28]. It will also affect the optimization of the difficulty of the corresponding problem. DTLZ1 and dtlz3 are mainly used to test the shrinkage performance of the algorithm, DTLZ2 and dtlz4 are mainly used to test the dispersion of the algorithm, DTLZS and dtlz6 are the exit problems, and the PF problem is segmented for DTLZ7. The attributes of the problem test in the DTLZ series are shown in Table 1 below.

#### 3.2.2. WFG series test problems

The WFG test problem toolbox not only includes a series of different problem feature functions, but also provides a set of design functions including structural geometry. We build a bottom-up algorithm through function tools, which has multiple features and controllable difficulty tests. The characteristics and related parameters of different problems in the WFG test are shown in Table 2 below.

#### 3.2.3. Evaluation index

The rotation generation distance IGD is expressed as the Pareto optimal solution set, the average distance between the indi-

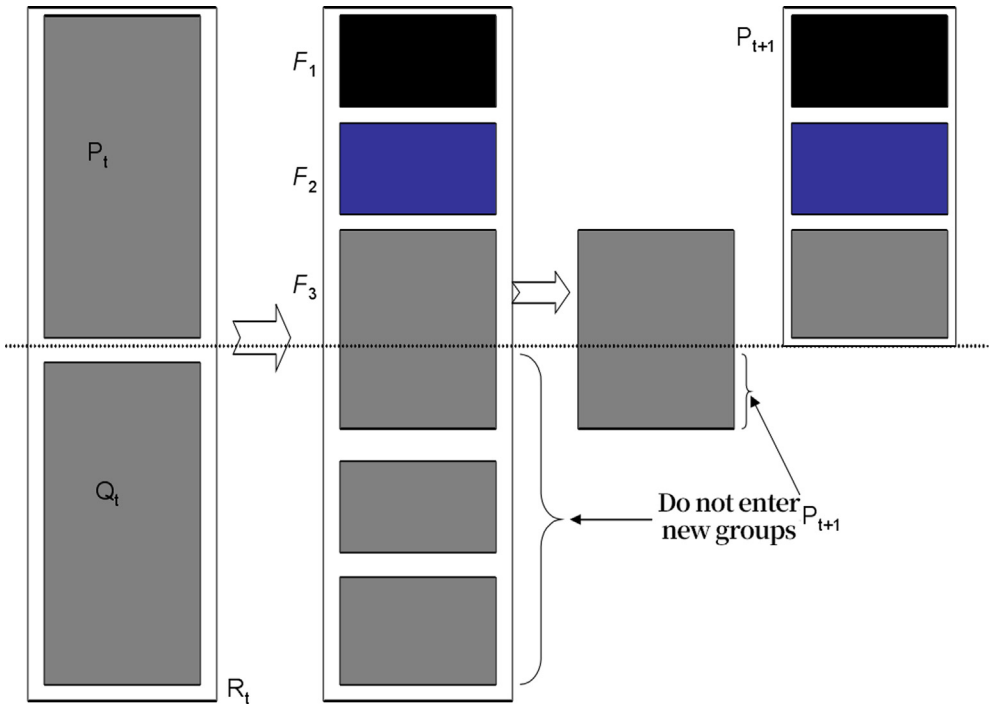


**Fig. 1** Schematic diagram of NSGA-II new group composition.

vidual in the real number PF* and the non-dominated solution set obtained by the algorithm. The formula is:

$$IGD = \frac{\sum_{j \in PF*} d_j'}{n} \tag{2}$$

The super large volume index HV has become an advanced evaluation index due to its excellent theoretical support. The comprehensive performance of MOEA is evaluated by using the hypervolume value of the closed space of the non-dominated solution set and the reference point (worst point). The formula is:

$$HV = \lambda\left(\bigcup\ i = 1|s|v_i\right) \tag{3}$$

In this paper, the expansion strategy is used to expand the richness of the population, accelerate the convergence efficiency of the algorithm, and artificially adjust the expansion strategy through the expansion rate r, thereby analyzing the effect of the expansion strategy on the algorithm. The influence of extending r on the extreme performance of Pareto is shown in Table 3.

### 3.3. Experimental results

#### 3.3.1. DTLZ series test problem test results

DS strategy can be combined with multi-objective evolutionary algorithms based on dominance relations. This paper combines the classic algorithms NSGA-II and SPEA2 with DS strategy based on the superiority relationship, and uses the DTLZ series of test questions to test and verify the DS strategy efficiency before and after the algorithm is added [29]. NSGA-II and SPEA2 have better performance on multi-objective low-dimensional optimization problems. DS is a strategy for multi-objective high-dimensional optimization problems. Therefore, this section uses DTLZ series of test problems in the three dimensions of 4, 5, and 6 Compare with experiment. Taking IGD as the evaluation index, the experimental results are shown in Table 4.

Fig. 3 and Fig. 4 are the optimization results of the four algorithms.

#### 3.3.2. Solving the multi-objective optimization model

First find the optimal solution for the first goal, find the set of all optimal solutions, and record it as R0; then find the optimal solution for the next goal in R0 and record it as R1; until the optimal solution x0 for m goals is obtained ,specifically is:

$$\begin{aligned} f_1(x^0) &= \underset{x \in R_0 \subset R}{Max} f_1(x) \\ f_1(x^0) &= \underset{x \in R_1 \subset R_0}{Max} f_2(x) \\ &\vdots \\ f_m(x^0) &= \underset{x \in R_{m-1} \subset R_{m-2}}{Max} f_m(x) \end{aligned} \tag{4}$$

Turn the multi-objective function into a single objective function, and then calculate the new objective function:

$$U(x) = \sum_{i=1}^{m} \lambda_i f_i(x) \tag{5}$$

If the requirements for different values are completely different between them, the following evaluation function can be used:

$$U(x) = \sum_{i=1}^{m} \lambda_i \left[f_i(x) - f_i^*\right]^2 \tag{6}$$

The best value for each goal:

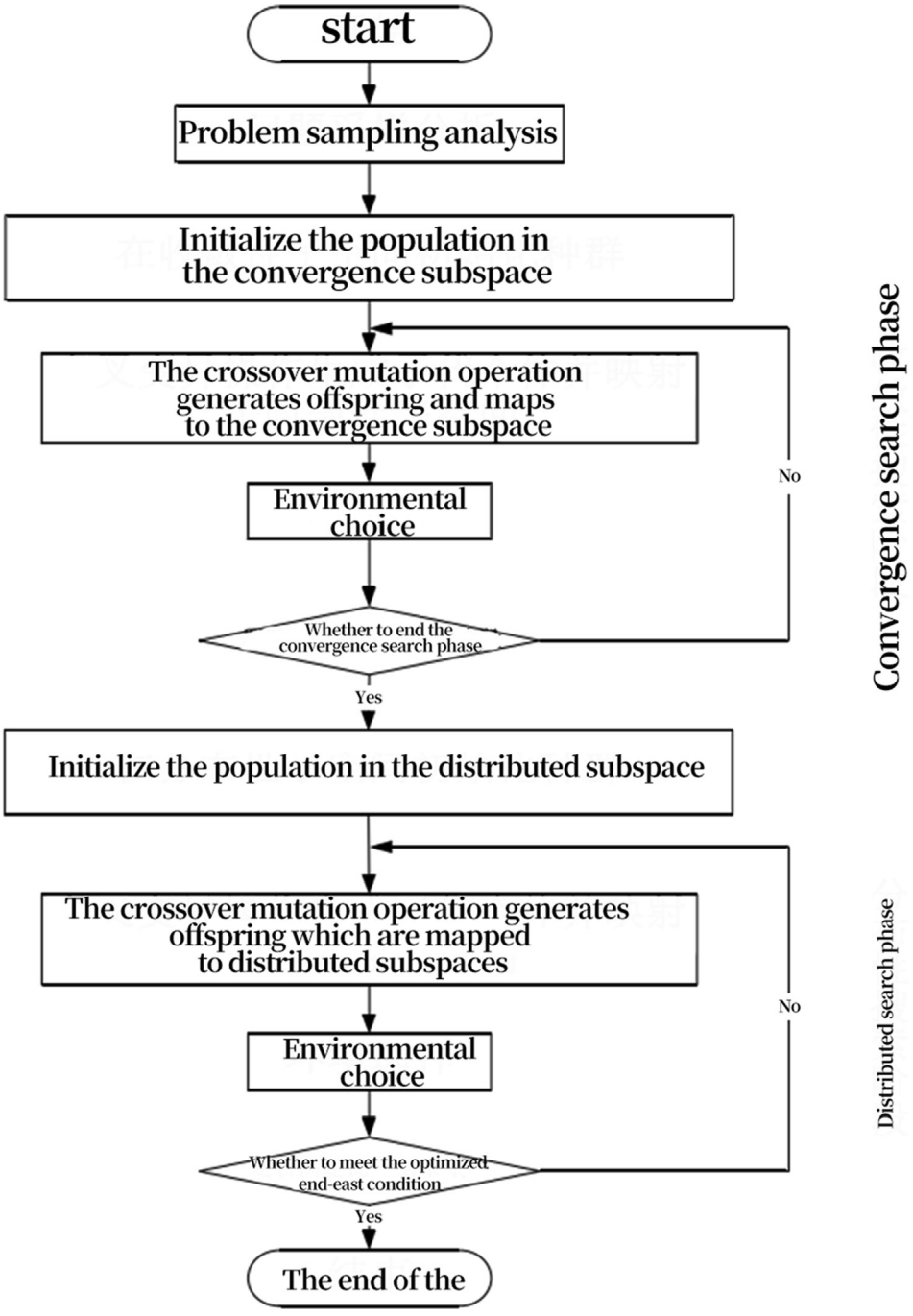


**Fig. 2** Algorithm flowchart.

$$f_0^i = \underset{x \in R}{Max} f_i(x) = f_i\left(x^{(i)}\right) \quad i = 1, 2, ..., m \tag{7}$$

Each goal can achieve its best point. Unfortunately, this is usually not possible, so the vector function:

$$F(x) = (f_1(x), f_2(x), ..., f_m(x))^T \tag{8}$$

$$F^0 = \left(f_1^0, f_2^0, ..., f_m^0\right)^T \tag{9}$$

The vector F is the ideal point. The ideal point method is to set a specific module. In this module, you must find a point as close to the ideal point as possible, that is, load the module:

$$\| F(x) - F^0 \| \to Min \| F(x) - F^0 \| \tag{10}$$

The meaning of the best point is different for different modules, and this module can also be an evaluation function. The general meaning of p-module is:

$$\| F(x) - F^0 \| = \left[ \sum_i^m \left(f_i^0 - f_i(x)\right)^p \right]^{1/p} = L_p(x) \tag{11}$$

The evaluation function can be used at this time:

$$U(x) = \frac{f_1(x) f_2(x) ... f_k(x)}{f_{k+1}(x) f_{k+2}(x) ... f_m(x)} \to \min \tag{12}$$

**Table 1** DTLZ test problem characteristics and parameter settings.

| Problem | Characteristic | Decision variable dimension (N) |
|---|---|---|
| DTLZ1 | Linear | M + 8 |
| DTLZ2 | Concave | M + 8 |
| DTLZ3 | Concave | M + 8 |
| DTLZ4 | Concave | M + 8 |
| DTLZS | Concave | M + 8 |
| DTLZ6 | Concave, deflection | M + 8 |
| DTLZ7 | Mixed, discontinuous | M + 8 |

Use their geometric mean:

$$D = \sqrt[m]{d_1 d_2 ... d_m} \tag{13}$$

### 3.4. Optimization method of multi-decision space decision network planning model

#### 3.4.1. Model identification analysis

This paper uses Gaussian process modeling to solve Q4-1, Q4-2, Q4-3 and Q4-4 problems with distance parameter models. Fig. 5 illustrates the uncertainty in the modeling interval.

Table 5 is the interval uncertainty Gaussian parameters; Table 6 is the interval midpoint Gaussian parameters.

#### 3.4.2. Interval optimization function identification

This article studies a series of optimization multi-objective problems. The m-objective function is:

$$f_m(x,u) = \left[\underline{f_m(x,u)}, f_m(\bar{x},u)\right], m = 1,2,...,z \tag{14}$$

The range number is the center point of the range and the range uncertainty. Interval security represents the correlation between the upper and lower limits of the interval, so the m-objective function is:

$$f_m(x,u) = [f_{cm}(x,u), f_{wm}(x,u)], m = 1,2,...,z \tag{15}$$

The interval proxy function is composed of the interval center point model and the uncertainty of the interval model, so the model data set is divided into two parts. The calculation formula is:

$$\begin{cases} D_{cm}^{learn} = \{(x_i, f_{cm}(x_i,u))\} \\ D_{wm}^{learn} = \{(x_i, f_{wm}(x_i,u))\} \end{cases}, i = 1,2,...,\zeta$$
$$X_1 = [x_1, ..., x_\zeta] \tag{16}$$
$$\begin{cases} F_{cm}^{learn} = [f_{cm}(x_i,u), ..., f_{cm}(x_\zeta,u)]^T \\ F_{wm}^{learn} = [f_{wm}(x_i,u), ..., f_{wm}(x_\zeta,u)]^T \end{cases}$$

The modeling method of interval uncertainty corresponds to the modeling method of the center point of the shooting range. In contrast, the modeling process of the scope center is relatively simple. The uncertainty of interval modeling, if the objective function relative to the output matrix is:

$$y_{wm} = [y_{wm}(x_1,u), ..., y_{wm}(x_\zeta,u)]^T \tag{17}$$

**Table 2** WFG test problem characteristics and parameter settings.

| Problem | Characteristic | Position parameter (k) | Distance parameter (l) |
|---|---|---|---|
| WFG1 | Convex, mixing, deflection | 3*(M−1) | 30 |
| WFG2 | Convex, no separation, discontinuity | 3*(M−1) | 30 |
| WFG3 | Linearity, no separation, degradation | 3*(M−1) | 30 |
| WFG4 | Concave, separated | 3*(M−1) | 30 |
| WFGS | Concave, separated | 3*(M−1) | 30 |
| WFG6 | Concave, no separation | 3*(M−1) | 30 |
| WFG7 | Concave, separated | 3*(M−1) | 30 |
| WFG8 | Concave, no separation | 3*(M−1) | 30 |

**Table 3** Pareto frontier performance indicators under different elongation rates.

| Stretch rate | | β = 0.2 | β = 0.4 | β = 0.6 | β = 0.8 | β = 1 |
|---|---|---|---|---|---|---|
| Q4-1 | E | 0.1314 | 0.1606 | 0.1848 | 0.1765 | 0.1796 |
| | D | 8.2872 | 8.1514 | 8.2609 | 8.2165 | 8.3558 |
| | C | 0.3387 | 0.3718 | 0.3736 | 0.3905 | 0.3751 |
| | E | 0.2978 | 0.3028 | 0.3075 | 0.3198 | 0.3288 |
| Q4-2 | D | 19.2334 | 19.4432 | 19.4289 | 19.3568 | 19.3521 |
| | C | 0.2695 | 0.2774 | 0.2857 | 0.2835 | 0.2811 |
| | E | 0.0418 | 0.0448 | 0.0458 | 0.4342 | 0.0392 |
| Q4-3 | D | 0.9944 | 0.9846 | 0.9868 | 1.0166 | 0.8973 |
| | C | 0.3063 | 0.3128 | 0.3073 | 0.3155 | 0.3105 |
| | E | 0.2953 | 0.3022 | 0.3143 | 0.3068 | 0.3149 |
| Q4-4 | D | 12.3705 | 12.4013 | 12.3275 | 12.4521 | 12.5022 |
| | C | 0.3005 | 0.3146 | 0.3248 | 0.3253 | 0.3107 |

**Table 4** Experimental results of DS-NSGA-II, NSGA-II, DS-SPEA2, SPEA2 on the DTLZ test problem.

| Test question | Target dimension | DS-NSGA-II | | NSGA-II | | DS-SPEA2 | | SPEA2 | |
|---|---|---|---|---|---|---|---|---|---|
| | | Mean | Variance | Mean | Variance | Mean | Variance | Mean | Variance |
| DTLZ1 | 4 | 0.0542(0.0000) | | 0.1302 t(0.0184) | | 0.0442(0.0000) | | 2.3884 t(12.9203) | |
| | 5 | 0.0748(0.0000) | | 7.5353 t(26.292) | | 0.0653(0.0000) | | 52.64 t(338.17) | |
| | 6 | 0.0898(0.0000) | | 19.99 t(481.33) | | 0.0828(0.0000) | | 112.42 t(717.09) | |
| DTLZ2 | 4 | 0.1348(0.0000) | | 0.1501 t(0.0001) | | 0.1202(0.0000) | | 0.1458 t(0.0001) | |
| | 5 | 0.18367(0.0001) | | 0.3418 t(0.0010) | | 0.1845(0.0002) | | 0.6154 t(0.0067) | |
| | 6 | 0.2802(0.0000) | | 1.0849 t(0.0415) | | 0.2672(0.0000) | | 1.4208 t(0.0607) | |
| DTLZ3 | 4 | 0.1347(0.0000) | | 49 t(262) | | 0.1242(0.0001) | | 33 t(155) | |
| | 5 | 0.1843(0.0001) | | 113 t(4148) | | 0.1892(0.0003) | | 306 t(7532) | |
| | 6 | 0.2811(0.0000) | | 159 t(6745) | | 0.2809(0.0000) | | 802 t(16085) | |
| DTLZ4 | 4 | 0.2258(0.0635) | | 0.1469 t0.000) | | 0.1978(0.0164) | | 0.3238 t(0.0615) | |
| | 5 | 0.2555(0.0125) | | 0.9678 t(0.0160) | | 0.2568(0.0225) | | 0.6426 t(0.0548) | |
| | 6 | 0.3921(0.0340) | | 1.8888 t(0.0126) | | 0.3847(0.0353) | | 1.4307 t(0.0993) | |
| DTLZ5 | 4 | 0.0077 t(0.0000) | | 0.0493 t(0.0001) | | 0.0802(0.0338) | | 0.1187 t(0.0007 | |
| | 5 | 0.0082 t(0.0000) | | 0.1018 t(0.0008) | | 0.0812(0.0347) | | 0.3787 t(0.0171) | |
| | 6 | 0.0084 t(0.0000) | | 0.1913 t(0.0108) | | 0.1116(0.0433) | | 1.2489 t(0.0740) | |
| DTLZ6 | 4 | 0.1012 t(0.0131) | | 3.3608 t(0.1604) | | 0.2346(0.2630) | | 2.2399 t(0.0261) | |
| | 5 | 0.2672 t(0.2390) | | 6.8339 t(0.3003) | | 0.3317(0.3200) | | 9.469 t(0.022 t) | |
| | 6 | 0.6109 t(0.6047) | | 7.8782 t(0.2310) | | 0.7066(0.9907) | | 9.9124 t(0.0008) | |
| DTLZ7 | 4 | 0.2165(0.0001) | | 0.2172 t(0.0001) | | 0.1758(0.0000) | | 0.1861 t(0.0013) | |
| | 5 | 0.3833(0.0001) | | 0.4384 t(0.0008) | | 0.3024(0.0002) | | 0.8031 t(0.002) | |
| | 6 | 0.8169(0.0001) | | 0.7285 t(0.0018) | | 0.4567(0.0001) | | 0.8428 t(0.0084) | |

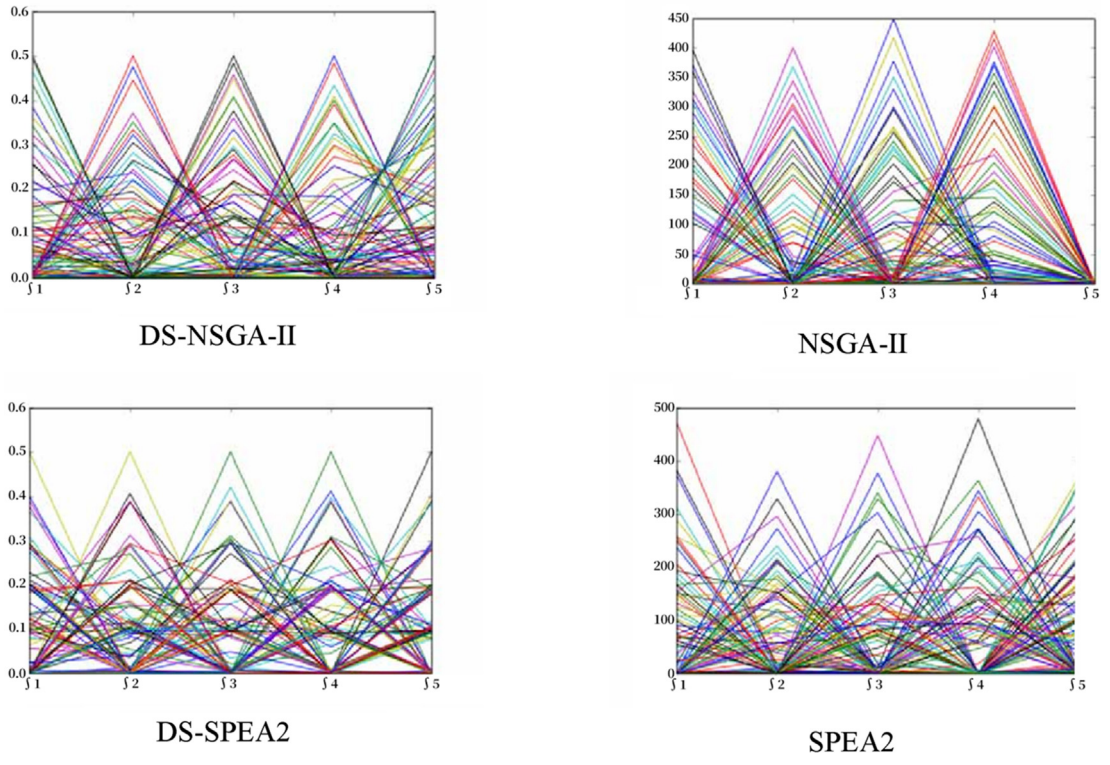


**Fig. 3** The experimental results of DS-NSGA-II, DS-SPEA2, NSGA-II, SPEA2 on DTLZ4 problem.

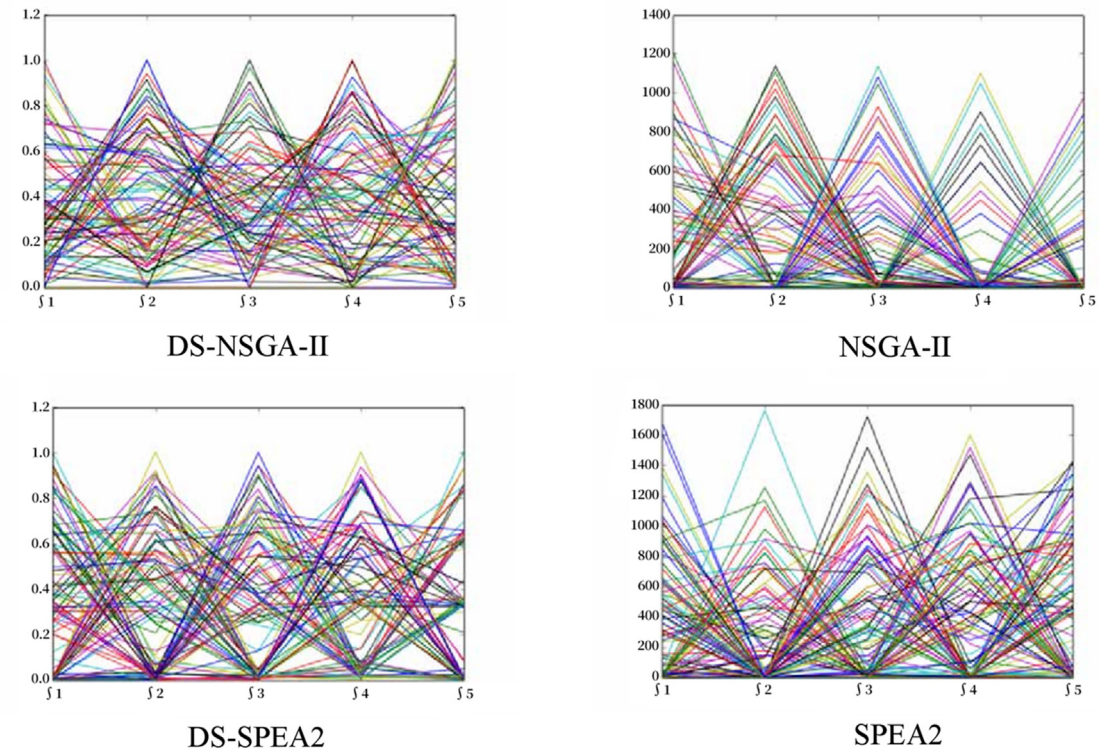


**Fig. 4** The experimental results of DS-NSGA-II, DS-SPEA2, NSGA-II, SPEA2 on DTLZ5 problem.

The final data set corresponding to the interval uncertainty function is determined that the variables in D obey the common Gaussian, which is:

$$f_{wm}(x_i,u)G\tilde{P}\big(e_{wm}(x_i),k_{wm}\big(x_i,x_j\big)\big) \tag{18}$$

If the covariance function is expressed in matrix form, it is:

$$C(X,X)=E\big[y_{wm}(x_i,u)y_{wm}^{T}(x_i,u)\big]=K(X,X)+\sigma_{wm}^{2}I \tag{19}$$

The Gauss-based proxy model should verify the accuracy of the model through the validation sample set.

$$\begin{cases} D_{cm}^{verify}=\{(x_i,f_{cm}(x_i,u))\} \\ D_{wm}^{verify}=\{(x_i,f_{wm}(x_i,u))\} \end{cases},i=1,2,...,\zeta^{*}$$
$$X_2=[x_1,...,x_{\zeta^{*}}] \tag{20}$$
$$\begin{cases} F_{cm}^{verify}=[f_{cm}(x_1,u),...,f_{cm}(x_{\zeta^{*}},u)]^{T} \\ F_{wm}^{verify}=[f_{wm}(x_1,u),...,f_{wm}(x_{\zeta^{*}},u)]^{T} \end{cases}$$

The observation starting value constituted by training and the observation output value constituted by verification should conform to the general Gaussian distribution, which is:

$$\begin{bmatrix} y_{wm}^{learn} \\ f_{wm}^{verity} \end{bmatrix}\tilde{\mathrm{N}}\left(\begin{bmatrix} \mu_{wm}^{learn} \\ \mu_{wm}^{verity} \end{bmatrix},\begin{bmatrix} C_{wm}(X_1,X_1)K_{wm}(X_1,X_2) \\ K_{wm}(X_2,X_1)K_{wm}(X_2,X_2) \end{bmatrix}\right) \tag{21}$$

A single input data should also meet the above characteristics, which are:

$$\begin{bmatrix} y_{wm}^{learn} \\ f_{wm}^{i} \end{bmatrix}\tilde{\mathrm{N}}\left(\begin{bmatrix} \mu_{wm}^{learn} \\ \mu_{wm} \end{bmatrix},\begin{bmatrix} C_{wm}(X_1,X_1)K_{wm}(X_1,x_i) \\ K_{wm}(x_i,X_1)K_{wm}(x_i,x_i) \end{bmatrix}\right) \tag{22}$$

Then get the Gaussian model proxy regression equation, which is:

$$e_{wm}^{*}(x_i)=\mu_{wm}+K_{wm}(x_i,X_1)\cdot C_{wm}(X_1,X_1)^{-1}\cdot\big(y_{wm}^{learn}-\mu_{wm}^{learn}\big) \tag{23}$$

$$\sigma_{wm}^{*}(x_i)^{2}=K_{wm}(x_i,x_i)-K_{wm}(x_i,X_1)\cdot C_{wm}(X_1,X_1)^{-1}\cdot K_{wm}(X_1,x_i) \tag{24}$$

The predicted output of the range center point obtained using the same method is:

$$e_{wm}^{*}(x_i)=\mu_{cm}+K_{cm}(x_i,X_1)\cdot C_{cm}(X_1,X_1)^{-1}\cdot\big(y_{cm}^{learn}-\mu_{cm}^{learn}\big) \tag{25}$$

The confidence level to reach the prediction is:

$$\sigma_{cm}^{*}(x_i)^{2}=K_{cm}(x_i,x_i)-K_{cm}(x_i,X_1)\cdot C_{cm}(X_1,X_1)^{-1}\cdot K_{cm}(X_1,x_i) \tag{26}$$

### *3.5. Comparison of Pareto frontier of improved algorithm and other algorithms*

Fig. 6 is the optimization range of the NSGA-II algorithm. The Pareto limit is obtained by solving the optimization problem, and the obtained limit has good symmetry and dispersion. Fig. 7 is the boundary comparison diagram of the NSGA-II algorithm and the improved algorithm. Table 7 shows the detailed measurement values of each algorithm.

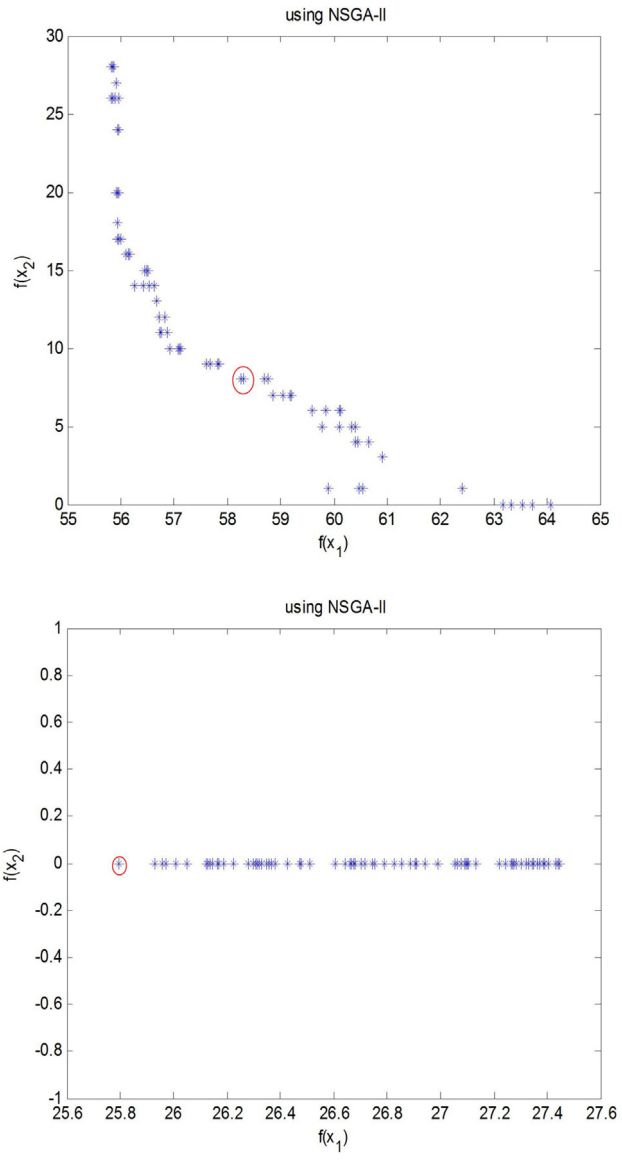


**Fig. 5** Q4-1: F1 interval uncertainty optimization diagram.

**Table 5** Interval uncertainty parameter set.

| Optimization | | Interval uncertainty parameter set $\omega_{wm}$ | | | |
|---|---|---|---|---|---|
| | | $v_{wm}$ | $\lambda_{wm}$ | $\sigma_{wm}$ | $\mu_{wm}$ |
| Q4-1 | $f_1$ | −8.008 | 60.785 | 0.132 | 0.963 |
| | $F_2$ | 6.302 | 10.874 | −0.019 | 0.542 |
| | $g_1$ | 2.864 | 38.271 | −0.003 | 0.412 |
| | $g_2$ | −1.093 | −40.563 | 0.175 | 0.873 |
| Q4-2 | $f_1$ | 3.012 | 67.908 | −0.638 | 0.598 |
| | $f_2$ | −3.226 | 55.126 | −0.251 | 1.405 |
| Q4-3 | $f_1$ | 3.337 | 16.421 | −0.203 | 0.365 |
| | $f_2$ | −2.542 | 32.626 | −0.053 | 1.175 |
| Q4-4 | $f_1$ | −0.568 | 31.874 | 0.968 | 1.039 |
| | $f_2$ | 0.668 | −61.548 | −0.054 | 0.648 |

**Table 6** Interval midpoint parameter set.

| Optimization | | Interval uncertainty parameter set $\omega_{cm}$ | | | |
|---|---|---|---|---|---|
| | | $v_{cm}$ | $\lambda_{cm}$ | $\sigma_{cm}$ | $\mu_{cm}$ |
| Q4-1 | $f_1$ | 6.703 | −75.758 | 0.036 | 0.073 |
| | $F_2$ | −3.172 | −65.861 | −0.034 | −0.087 |
| | $g_1$ | −5.566 | −75.847 | 0.842 | 0.009 |
| | $g_2$ | 2.561 | 79.847 | −1.041 | 0.766 |
| Q4-2 | $f_1$ | 5.715 | 62.115 | −0.098 | 0.585 |
| | $f_2$ | 20.989 | −72.396 | −0.042 | 1.128 |
| Q4-3 | $f_1$ | 5.908 | 40.855 | 0.103 | 1.395 |
| | $f_2$ | 17.371 | −45.413 | 0.004 | 1.144 |
| Q4-4 | $f_1$ | 1.674 | −4.023 | 1.602 | 0.422 |
| | $f_2$ | −0.788 | 72.815 | −0.117 | 1.022 |

## 4. Research on simulation control of sports training based on directional search in decision space

### *4.1. The overall design of the sports training simulation system*

#### *4.1.1. Simplified model of human in sports training simulation system*

Joints play a major role in the upper and lower parts of the human body. So we need to keep the shoulder, elbow, and wrist joints on the upper limbs, and the hip, knee, and ankle joints on the lower limbs. Details are shown in Table 8.

#### *4.1.2. Hierarchy*

In order to create a skeletal motion model that conforms to the human body, it is necessary to introduce the connected limbs in the model and the common relationship between these limbs. This article regards the joints in the model as points and the bones between the joints as chains, so that the model can connect limbs according to the motion relationship. By using a number as the root node of two adjacent joints, the joint near the number node should be the parent node, and the joint below the parent node should be the child node. When the parent node moves, the bottom node should move with it. But when the child node moves, the parent node does not necessarily move. The details are shown in Fig. 8.

### *4.2. Multi-objective optimization of virtual human walking motion generation*

Reusing the obtained data to synthesize different actions has always played a major role in the generation of virtual human actions. It usually includes two methods: creating a sports library, directly editing and synthesizing data; using machine learning technology to build a sports data model, and using the model to generate a variety of new sports, and virtual human activity generation technology based on PCA and ICA. The details are shown in Fig. 9 below:

#### *4.2.1. Generation of PCA space*

In order to move the coordinate connection to the data center, the tho vector is defined as the average sector of all n-dimensional i vectors in the motion matrix M. Therefore, the

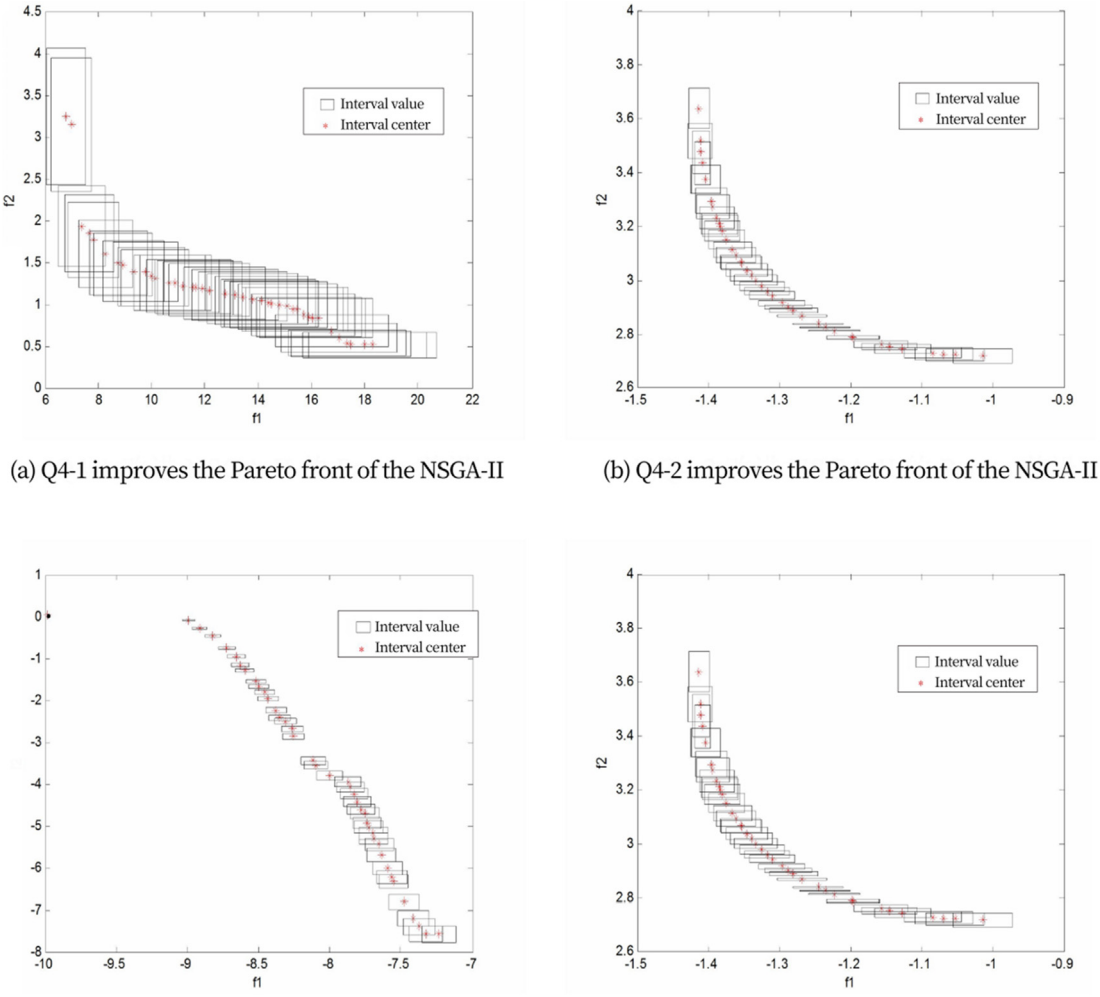


**Fig. 6** Improve the Pareto frontier of NSGA-II.

basic sector of the entire space is the tilt vector i composed of m orthogonal principal components, and the formula is:

$$\theta \cong \theta_0 + \sum_{i=1}^{m} \alpha_i e_i = \theta_0 + \alpha E \tag{27}$$

PCA analysis considers all data of all samples, and its main components are compact. Therefore, a simple cleavage method is used to decompose it into the main component space of each sample. Therefore, the formula of the coefficient matrix (a)i related to the sample (v) is:

$$\alpha \cong \alpha_0 + \sum_{i=1}^{n} \beta_i f_i = \alpha_0 + \beta F_v \tag{28}$$

The formula is based on minimizing:

$$\sum_{j=1}^{nbs} \left(\alpha_{ij} - d_{ij}\right)^2 = \sum_{j=1}^{nbs} \left(\alpha_{ij} - m_i s_i - b_i\right)^2 \tag{29}$$

#### 4.2.2. System model driven design

The basic framework of the simulated population is shown in Fig. 10.

### 4.3. Realization of simulation system

#### 4.3.1. System function

(1) Real simulation of three-dimensional technical actions. Through the visualization method, the athletes can understand the essence of technical movements more conveniently and quickly, thereby improving the overall level of the athletes. This technique can be used not only in daily training, but also in training referees.
(2) New sports design and technical sports standardization. Able to organize, create and modify some new actions. With this tool, trainers can also formulate their own "ideal" actions. And based on this, create a library of referee education and training standard actions to improve the effect of the game.
(3) Technical movement analysis. Able to perform technical quantitative analysis of the action, and the analysis situation can also be graphically displayed. And based on this, the "ideal" movement and the athlete's technical movement are compared in detail, which can help the

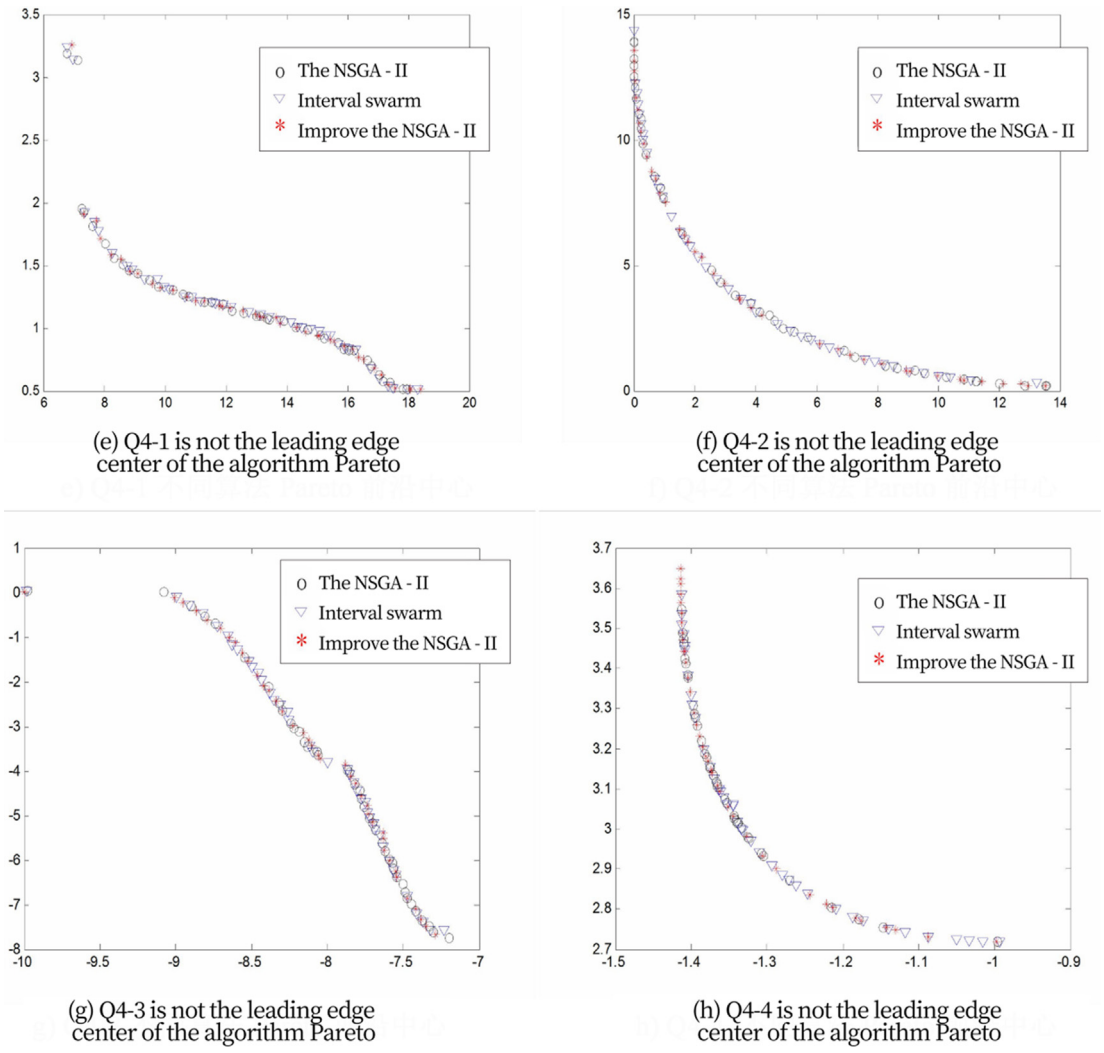


**Fig. 7** Pareto Frontier Center of Different Algorithms.

**Table 7** Algorithm comparison.

| Optimization function | NSGA-II algorithm | | Interval particle swarm optimization | | Interval NSGA-II algorithm | |
|---|---|---|---|---|---|---|
| | E measure | D measure | E measure | D measure | E measure | D measure |
| Q4-1 | 0.2233 | 11.8131 | 0.2237 | 11.9293 | 0.2518 | 12.4441 |
| Q4-2 | 0.3596 | 19.3885 | 0.3157 | 19.3209 | 0.2391 | 19.5373 |
| Q4-3 | 0.1608 | 8.2499 | 0.1458 | 8.1769 | 0.1302 | 8.3659 |
| Q4-4 | 0.0436 | 0.9533 | 0.0168 | 1.0137 | 0.0328 | 1.0463 |

athlete improve the technical ability and level of the movement.

(4) Technical operation analysis. Able to perform quantitative technical analysis of actions, and the analysis can be displayed graphically. Including displacement, efficiency, power, etc. Based on this, we will conduct in-depth research on "ideal" movements and athletes' technical movements, and provide suggestions and opinions for athletes to improve their level of movement.

(5) Simulation of center of gravity trajectory. It can analyze the overall technical movements of the athletes, simulate the changing trajectory of the center of gravity, and help coaches to comment on the technical movements of the athletes and improve the training level of the athletes.

(6) Comparison of simulation results and training videos. By displaying athletes' training actions and simulated actions on the same screen, and comparing them with the same perspective and synchronization, coaches and

**Table 8** Definition of joints and bones of virtual human simplified model.

| Joint definition | Attached to bone |
|---|---|
| Waist joint | Pelvic bones |
| Chest joint | Lumbar bone |
| Knee joint | Tibia bone |
| Shoulder joint | Upper arm bones |
| LOL | Hand bones |
| Neck spine | Spine bones |
| Marrow joint | Femur bone |
| Step on the joint | Calcaneus bone |
| Elbow joint | Forearm bones |

athletes can analyze the differences in actions, help athletes find technical deficiencies and improve them, and improve their training level.

(7) Action scheduling simulation and plan. In the imitated personal actions, the coach chooses the actions to be arranged. The system simulates the game situation according to the coach's choice. The coach can choose the best arrangement from a variety of results and help the coach develop a training plan.

#### *4.3.2. Simplified scheme of freedom of movement*

The degree of freedom of motion is related to the complexity of the problem to a certain extent, because the degree of freedom of motion usually requires a motion equation to express. The model established in this paper has 34 degrees of freedom. See Table 9 for details (Table 10.Table 11.Table 12.Table 13.)

#### *4.3.3. Implementation of database tables*

The tables in the database are mainly:

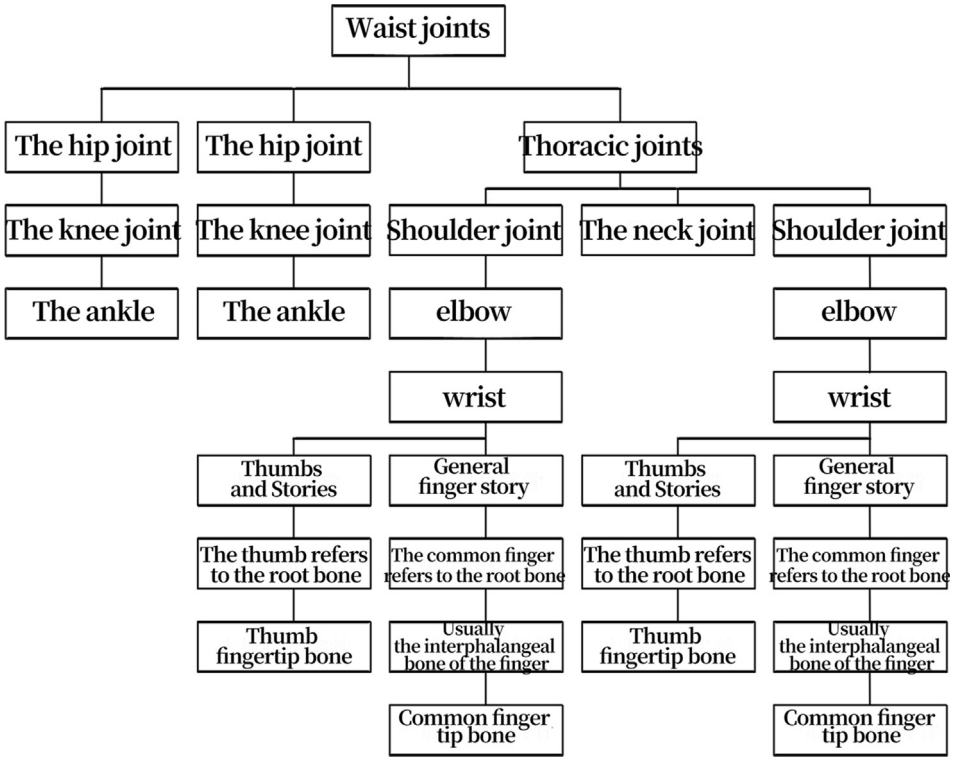


**Fig. 8** The hierarchy of virtual people in this article.

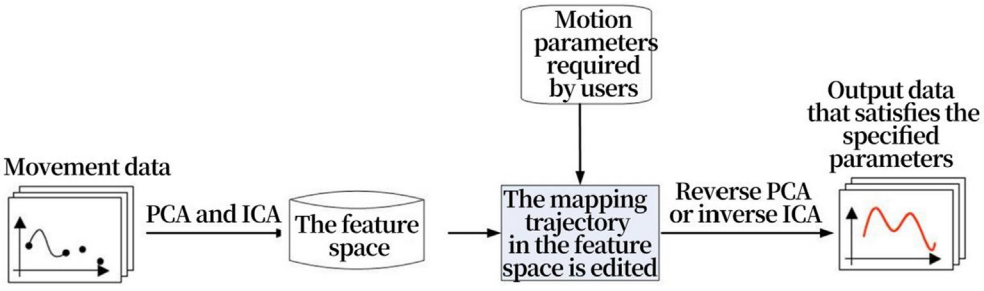


**Fig. 9** PCA-based or ICA-based motion generation process.

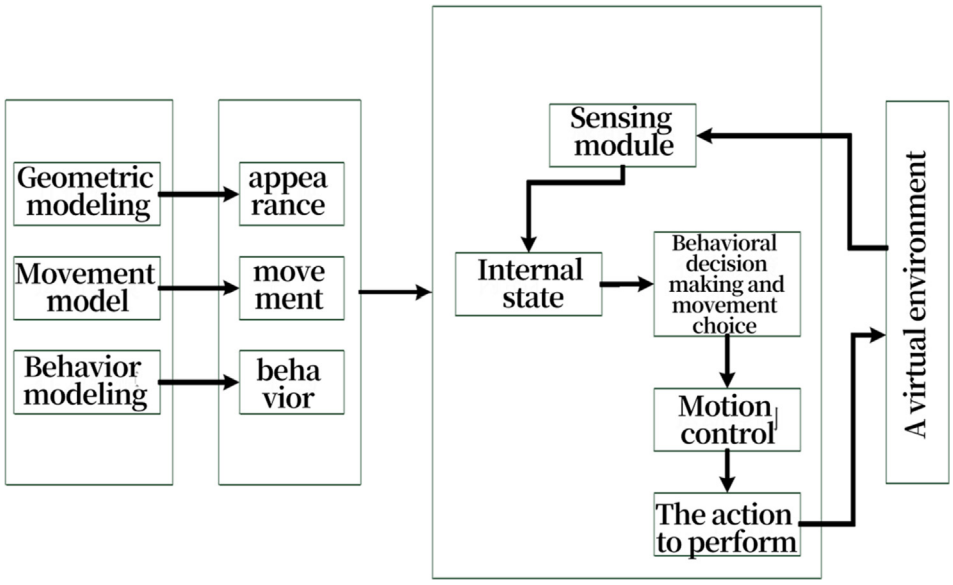


**Fig. 10** Motion structure frame of virtual people and virtual crowds.

(1) The basic physical condition of the athlete.
(2) The height and weight of athletes.
(3) The athlete's grip strength.
(4) Sports item evaluation form, to evaluate sports items.

### *4.4. Suggestions on digital control of sports training simulation*

According to the relevant daily training situation and competition situation, the digital management system for athletes training can help athletes improve their sports level. However, since the physical condition of each remote mobilization is not exactly the same, the physical growth level of each sports park is not exactly the same. In addition, there are gradual differences in the physical conditions of individual athletes. This phenomenon has a lot to do with the changes in athletes' psychological conditions during daily training, and also has a lot to do with the pertinence and effectiveness of the training program. It is necessary to train athletes to strengthen their physical indicators, and at the same time strengthen the management and control of sports training management data, add high-tech management and control methods, and conduct scientific training. In addition, it is necessary to carry out targeted training and intervention according to the athlete's individual situation and psychological quality, so that the athlete can maintain a healthy and upward training and competition state.

**Table 9** Freedom of movement of virtual human.

| Joint | Axis of rotation | Maximum movement angle (.) |
|---|---|---|
| Waist joint | X | −46–90 |
| | Y | −50–60 |
| | Z | −56–56 |
| Hip joint | X | −166–46 |
| | Y | −30–30 |
| | Z | −130–30 |
| Knee joint | X | 0–166 |
| Ankle joint | X | −46–50 |
| | Z | 0–36 |
| Neck joint | X | −60–90 |
| | Y | −80–90 |
| | Z | −70–60 |
| Chest joint | X | −60–100 |
| | Y | −50–56 |
| Shoulder joint | X | −90–180 |
| | Y | −90–160 |
| | Z | −90–100 |
| Elbow joint | X | −90–50 |
| | Y | 0–130 |
| LOL | X | −46–46 |
| | Z | −80–80 |

## 5. Conclusion

This paper points out a single decision structure that can express multiple decision spaces, and adds sports training data to the network, and studies the multi-decision network planning model. It can be seen that the biggest advantage of this method is that it can express multiple decision spaces in a network in a relatively short form, so that managers have a clear understanding of the significant differences between each set of options that may occur. It is practical for managers and can choose from the macro level from the overall perspective of the project. This paper focuses on the study of the combination of metrics between attributes, and uses the theory of multi-attribute functions to combine ideal points to create multi-objective model conversion and solutions. This method can better overcome the multimedia difficulties in multi-decision network planning, and is used to improve and optimize projects. An efficient method is proposed.

**Table 10** Athlete Basic Information Sheet.

| Field meaning | Field Name | Field Type | Primary key |
|---|---|---|---|
| Numbering | Nume | nvarechar(50) | Is the primary key |
| Name | nam | nvarechar(50) | Not a primary key |
| Gender | sex | nvarechar(50) | Not a primary key |
| Date of birth | birtheday | datetime | Not a primary key |
| Body weight | Weighte | floate | Not a primary key |
| Height | Heighte | floate | Not a primary key |
| Vital capacity | vital_capaecity | floate | Not a primary key |
| Heart rate | Heartbat | inte | Not a primary key |
| Systolic blood pressure | prssor_pressure | floate | Not a primary key |
| Diastolic blood pressure | extending_prssure | floate | Not a primary key |
| Sprint | sprinte | floate | Not a primary key |
| Grip | Gripe | floate | Not a primary key |
| Middle and long distance running | Ruunning | floate | Not a primary key |
| Seat body forward bending | seat_pronenes | floate | Not a primary key |

**Table 11** Height to weight ratio evaluation form.

| Field meaning | Field Name | Field Type | Primary key |
|---|---|---|---|
| Rule number | nume | nchar(10) | Is the primary key |
| Minimum height | Heighte_lowerlimite | floate | Not a primary key |
| Maximum height | heighte_upperlimite | floate | Not a primary key |
| Lower weight limit | weighte_lowerlimite | floate | Not a primary key |

**Table 12** Grip strength evaluation form.

| Field meaning | Field Name | Field Type | Primary key |
|---|---|---|---|
| Rule number | nume | nchare(10) | Is the primary key |
| Lower limit of grip | Gripe_lowerlimite | floate | Not a primary key |
| Upper limit of grip | Gripe_upperlimite | floate | Not a primary key |
| Grip Index | Gripe_index | floate | Not a primary key |
| Grip strength | Gripe_sstatus | nchare(10) | Not a primary key |
| Percentage of grip | scale | floate | Not a primary key |

**Table 13** Grip strength evaluation form.

| Field meaning | Field Name | Field Type | Primary key |
|---|---|---|---|
| Sport name | Sporte_name | nvarchare(50) | Is the primary key |
| Power | powere | inte | Not a primary key |
| Speed | sped | floate | Not a primary key |
| Endurance | staminae | floate | Not a primary key |
| Agility/flexibility | flexibilitye | floate | Not a primary key |

## Declaration of Competing Interest

The authors declare that they have no known competing financial interests or personal relationships that could have appeared to influence the work reported in this paper.

## Acknowledgement

This work was supported by Xiangyang Science & Technology Plan (High-tech field, GrantNo. 2020ABH001191), Hubei University of Arts and Science Scientific Research Starting

Foundation (Grant No. 2059073 & 2059074), The Basic Soft Science Research Projects of Wenzhou Science and Technology Bureau (Grant No. R20180012), The Zhejiang Philosophyand Social Sciences Foundation (Grant No. 19NDJC145YB), and Zhejiang Public WelfareTechnology Application Research Project (Grant No. LGG19F020004).

## References

[1] V. Renò, N. Mosca, M. Nitti, et al, A technology platform for automatic high-level tennis game analysis, Comput. Vision Image Understand 15 (9) (2017) 462–475.
[2] D.T. Nguyen, J.E. Jung, Real-time event detection for online behavioral analysis of big social data, Future Gener. Comput. Syst 1 (66) (2017) 137–145.
[3] A. Ravi, H. Venugopal, S. Paul, H.R. Tizhoosh, A dataset and preliminary results for umpire pose detection using SVM classification of deep features, in: In: 2018 IEEE Symposium Series on Computational Intelligence (SSCI), 2018, pp. 1396–1402.
[4] V. Ellappan, R. Rajasekaran, Event recognition and classification in sports video, in: In: 2017 Second International Conference on Recent Trends and Challenges in Computational Models (ICRTCCM), 2017, pp. 182–187.
[5] P. Shukla, H. Sadana, A. Bansal, et al, Automatic cricket highlight generation using event-driven and excitement-based features, in: In: Proceedings of the IEEE Conference on Computer Vision and Pattern Recognition Workshops, 2018, pp. 1800–1808.
[6] A. Javed, Event driven video summarization for sports, University of Engineering and Technology, Taxila, Pakistan, PhD diss., 2016, pp. 764–779.
[7] M.H. Kolekar, S. Sengupta, Bayesian network-based customized highlight generation for broadcast soccer videos, IEEE Trans. Broadcast 61 (2) (2015) 195–209.
[8] A. Baijal, J. Cho, W. Lee, B.-S. Ko, Sports highlights generation based on acoustic events detection: a rugby case study, in: In: 2015 IEEE International Conference on Consumer Electronics (ICCE), 2015, pp. 20–23.
[9] J. Zhang, J. Yao, X. Wan, Towards constructing sports news from live text commentary. In: Proceedings of the 54th Annual Meeting of the Association for Computational Linguistics (Volume 1: Long Papers), vol 54(1) (2016), 1361–1371.
[10] A. Bhalla, A. Ahuja, P. Pant, A. Mittal, A multimodal approach for automatic cricket video summarization, in: In: 2019 6th International Conference on Signal Processing and Integrated Networks (SPIN), 2019, pp. 146–150.
[11] S.K. Baliarsingh, S. Vipsita, K. Muhammad, S. Bakshi, Analysis of high-dimensional biomedical data using an evolutionary multi-objective emperor penguin optimizer, Swarm Evolut. Comput 48 (2019) 262–273.
[12] Z. Xing, An improved emperor penguin optimization based multilevel thresholding for color image segmentation, Knowl.-Based Syst 194 (2020) 105–170.
[13] A. Javed, S.A. Irtaza, H. Malik, et al, A multimodal framework based on audio-visual features for summarization of cricket videos, IET Image Proc 13 (4) (2019) 615–622.
[14] M.H. Kolekar, Bayesian belief network-based broadcast sports video indexing, Multimedia Tools Appl 54 (1) (2011) 27–54.
[15] M. Nasir, A. Javed, A. Irtaza, et al, Event detection and summarization of cricket videos, J. Image Graphics 6 (2018) 27–32.
[16] K. Midhu, N.A. Padmanabhan, Highlight the generation of cricket matches using deep learning. In: Computational Vision and Bio Inspired Computing (2018), 925–936.
[17] S. Chakraborty, D. Thounaojam, A novel shot boundary detection system using hybrid optimization technique, Appl. Intell 49 (03) (2019) 721–736.
[18] A. Javed, K.B. Bajwa, H. Malik, et al, A hybrid approach for summarization of cricket videos, in: In: 2016 IEEE International Conference on Consumer Electronics-Asia (ICCE-Asia), 2016, pp. 1–4.
[19] M.H. Kolekar, S. Sengupta, Semantic concept mining in cricket videos for automated highlight generation, Multimedia Tools Appl 47 (3) (2010) 545–579.
[20] R. Hari, M. Wilscy, Event detection in cricket videos using intensity projection profile of Umpire gestures, in: In: 2014 Annual IEEE India Conference (INDICON), 2014, pp. 1–6.
[21] M. Merler, K.-N.C. Mac, D. Joshi, et al, Automatic curation of sports highlights using multimodal excitement features, IEEE Trans. Multimedia 21 (2019) 1147–1160.
[22] F. Hajati, M. Tavakolian, Video Classification Using Deep Autoencoder Network 15 (01) (2020) 508–518.
[23] G. Dhiman, V. Kumar, Emperor penguin optimizer: a bio-inspired algorithm for engineering problems, Knowl.-Based Syst 159 (2018) 20–50.
[24] P. Heckbert, Color image quantization for frame buffer display, SIGGRAPH Comput. Graph 16 (3) (1982) 297–307.
[25] G. Joy, Z. Xiang, Center-cut for color-image quantization, Vis. Comput 10 (1) (1993) 62–66.
[26] R. Balasubramanian, J.P. Allebach, C.A. Bouman, Color-image quantization with use of a fast binary splitting technique, J Opt Soc Am A 11 (11) (1994) 2777–2786.
[27] D. Clark, The popularity algorithm, Dr Dobb's J (1995) 121–127.
[28] S.J. Wan, S.K.M. Wong, P. Prusinkiewicz, An algorithm for multidimensional data clustering, ACM Trans. Math. Softw 14 (2) (1988) 153–162.
[29] M. Gervautz, W. Purgathofer, A simple method for color quantization: Octree quantization, in: New trends in computer graphics, Springer, Berlin, 1988, pp. 219–231.